Necessity of self-energy corrections in LEED theory for Xe(111): Comparison between theoretical and experimental spin-polarized LEED data

G. Hilgers,* M. Potthoff,† N. Müller, and U. Heinzmann
Fakultät für Physik, Universität Bielefeld, D-33501 Bielefeld, Germany

L. Haunert, J. Braun, and G. Borstel
Fachbereich Physik, Universität Osnabrück, D-49069 Osnabrück, Germany
(Received 27 February 1995)

An essential problem in calculating the electronic structure of solids is that created by many-body interactions. They cause self-energy corrections which in insulators and semiconductors range up to the width of the fundamental band gap. Angular-dependent intensity and asymmetry profiles measured in spin-polarized low-energy electron diffraction (SPLEED) from Xe(111) clearly show the necessity of the self-energy correction if compared to standard SPLEED calculations. Effects due to the self-energy correction have to be clearly distinguished from effects due to the inner potential. The real part of the inner potential affects the energy and, by refraction at the surface potential barrier, the angles of the incident and the diffracted beams, whereas the self-energy correction is equivalent to a change of the energy of the primary beam only. This qualitative difference is proved in our SPLEED investigations and is used to determine the self-energy correction and the inner potential from angular-dependent profiles. For the self-energy correction we found a value of $\Delta E = 3.0 \pm 1.5$ eV and for the real (imaginary) part of the inner potential $V_{0r} = 3.0 \pm 1.5$ eV ($V_{0i} = 2.0 \pm 0.5$ eV).

INTRODUCTION

The diffraction of low-energy electrons (LEED) at surfaces exhibits a strong sensitivity to structural parameters. This is the main reason for the success of this method in the determination of the geometric structure of clean and adsorbate-covered surfaces. However, electron diffraction at surfaces is not only sensitive to geometric parameters, but also to parameters characterizing the electronic structure.

The electronic structure (band structure) of the target above the vacuum level is known to be closely connected with the intensity of the diffracted electron beams in LEED.[1–4] The band structure contains information about the bulk density of electronic states depending on wave vector and energy. Minima in the intensity of the diffracted beams should occur for energies and wave vectors where electronic states with a high density of states couple to the wave function of the incident electron: the incident electron can penetrate deeply into the crystal, and the probability of reflection at the surface is low. On the other hand, the intensity of the diffracted electron beams should have a maximum for energies or wave vectors connected with a vanishing density of states, i.e., in band gaps; in this situation the incident electrons cannot couple to any electronic states and thus cannot penetrate into the crystal. Thus varying the energy and angle of incidence of the primary electron beam, the crystal band structure above the vacuum level can be studied by LEED.

Such a study has been carried out successfully in very-low-energy electron diffraction (VLEED):[5] the (111) surfaces of several fcc crystals show band gaps affecting the intensity of the diffracted electron beams in the way described above; in addition, critical points of the band structure like forbidden band crossings manifest themselves as sharp maxima with respect to the energy and the angle of incidence. A surface state, also contributing to the electronic density of states of the semi-infinite system, can be observed directly, when the energy of the states lies in a band gap.[6] Here the surface state produces a sharp minimum in a broad maximum of the intensity of the diffracted electron beam. The energy bands in a solid are energetically split as a consequence of the spin-orbit interaction. Thus with spin-polarized LEED spin-dependent effects also should be observed.

The objective of this paper is to demonstrate that the sensitivity with respect to electronic parameters also qualifies (spin-polarized) LEED for investigating many-body effects. Accounting for many-body effects in the theoretical analysis is inevitable, especially for typical transition metals such as Ni.[7–10] But many-body interactions may also be quite important for semiconductors and insulators. In the study presented here a Xe crystal was chosen as a prototype of an insulator. It is well known that for insulators it is particularly the width of the fundamental band gap which is affected by many-body interactions. Usually the width of the band gap is underestimated by band-structure calculations that are based on the density-functional theory (DFT). With respect to the band gap, the local-density approximation (LDA) is not sufficient for a correct description of the effects due to electron correlations. Band-structure calculations based on DFT-LDA (Refs. 11–13) predict a band gap of 5.5–7 eV. Optical reflection and absorption measurements[14–17] result in an approximately 3 eV larger band gap of 9.3 eV. The difference ΔE obviously is a consequence of

many-body interactions that have not been accounted for by the LDA, and thus will be termed as a self-energy correction in the following. This self-energy correction ΔE is independent of wave vector and energy since, apart from a constant shift, the unoccupied part of the Xe band structure is well described by the DFT-LDA formalism.

The self-energy correction ΔE can be obtained independently by means of a LEED analysis comparing measured and corresponding calculated LEED profiles: commonly, LEED calculations are based on a (muffin tin) potential model, which results from band-structure calculations within DFT-LDA. Therefore, the calculated LEED profiles correspond to a calculated DFT-LDA band structure, and consequently they have to be corrected with respect to many-body interactions; i.e., the self-energy correction ΔE also has to be taken into account in the calculation of LEED profiles.

If the dependence on wave vector and energy is allowed to be neglected, there is an easy way of introducing the self-energy correction ΔE in the LEED calculation, since the energy of the primary electron beam merely has to be corrected by the amount of ΔE: if E_{expt} denotes the kinetic energy of the primary electron beam in the experiment, then the calculation should be carried out for an energy E_{VL} that is given by (see Fig. 1)

$$E_{\text{VL}}=E_{\text{expt}}-\Delta E \ . \tag{1}$$

For an accurate determination of ΔE from the comparison between measured and calculated profiles, an energy range has to be chosen where the profiles are strongly energy dependent.

However, another important point has to be considered. The self-energy correction ΔE has to be determined simultaneously with another energy-correcting parameter, the real part V_{0r} of the inner potential. V_{0r} is the energetic height of the surface barrier, i.e., the energy difference between the vacuum level and the muffin-tin zero of the muffin-tin potential. Considering additionally the correction due to V_{0r}, the following results (see Fig. 1):

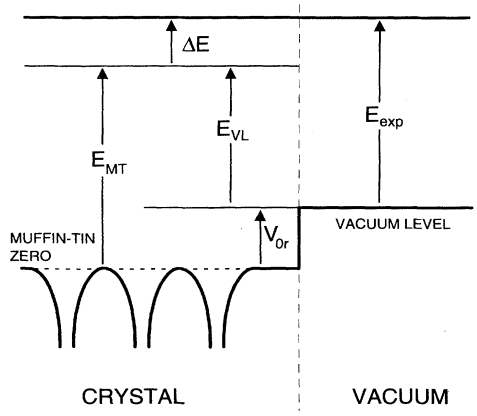

FIG. 1. Energies and potentials in electron diffraction. See text for key to symbols.

$$E_{\text{MT}}=E_{\text{VL}}+V_{0r}=E_{\text{expt}}-\Delta E+V_{0r} \ . \tag{2}$$

Here E_{MT} denotes the energy of the primary beam inside the crystal with respect to the muffin-tin zero. The intensity of the outgoing diffracted beams are exclusively determined by the value of E_{MT} in the calculation. Thus there are two *a priori* unknown parameters ΔE and V_{0r}, which both appear as additive constants that correct the kinetic energy in the experiment E_{expt} to obtain E_{MT}.

For normal incidence of the primary beam and recording only energy-dependent profiles of the diffracted beams, which is typical for conventional LEED, there is no way of distinguishing between the effects of the self-energy correction ΔE and the real part V_{0r} of the inner potential. Only the difference $\Delta E-V_{0r}$ can be determined by the comparison between measured and calculated profiles. Mostly, a self-energy correction is not considered at all and all energy-correcting terms are assumed to be included in the real part V_{0r} of the inner potential.

Only if there are significant effects due to the refraction of the beams at the surface barrier, can information about V_{0r} and ΔE be obtained separately. In the case of normal incidence, only the nonspecular diffracted beams are refracted at the surface barrier. To determine V_{0r} as well as ΔE, not only the profiles have to be recorded but also the angular positions of the diffracted beams must be controlled carefully in the experiment. In the case of off-normal incidence, however, it is also the primary beam and the specular diffracted beam that undergo a refraction at the surface barrier. The refraction is described by

$$\begin{aligned}\sin\vartheta_i &= \sin\vartheta \left[\frac{E_{\text{expt}}}{E_{\text{expt}}+V_{0r}}\right]^{1/2} \\ &= \sin\vartheta \left[\frac{E_{\text{MT}}+\Delta E-V_{0r}}{E_{\text{MT}}+\Delta E}\right]^{1/2} \ .\end{aligned} \tag{3}$$

In this equation ϑ means the polar angle outside the crystal, and ϑ_i means the polar angle inside the crystal after refraction. The refraction at the surface barrier is due exclusively to the real part V_{0r} of the inner potential but not due to the self-energy correction ΔE. Therefore, the effects of V_{0r} and ΔE can be distinguished easily at $\vartheta\neq 0$.

This is illustrated in Fig. 2, where the refraction at the surface barrier is illustrated schematically for the incident beam and the specular diffracted beam. The two parameters ΔE and V_{0r} are varied in such a manner that the difference $\Delta E-V_{0r}$ and thus E_{MT} remain unchanged [see Eq. (1)]. Additionally, according to Eq. (3), the value of the polar angle ϑ has been varied in such a way that ϑ_i remains unchanged as well. The different situations shown in Fig. 2 must result in identical (spin-dependent) intensities of the outgoing beam in the calculation, since the energy E_{MT} and the angle of incidence of the primary beam after refraction, i.e., inside the crystal, remain constant. Therefore, considering a polar-angle-dependent intensity or asymmetry profile [the asymmetry is obtained from the spin-dependent intensities; see Eq. (4) below], variations of ΔE and V_{0r} with $\Delta E-V_{0r}=\text{const}$ do not affect the profile in general but only the angular positions of its structures. Only for the correct combination of

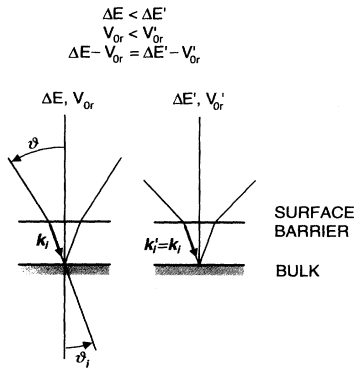

FIG. 2. Change of the refraction at the surface barrier for the specular beam keeping $\mathbf{k}_i$, i.e., ϑ_i and E_{MT}, constant and varying the self-energy correction ΔE and the real part V_{0r} of the inner potential such that $\Delta E - V_{0r} = \Delta E' - V'_{0r}$.

both ΔE and V_{0r} can reasonable agreement of measured and calculated profiles be expected. As a conclusion, for off-normal incidence not only the difference $\Delta E - V_{0r}$ but both ΔE and V_{0r} can be determined from the analysis of polar-angle-dependent intensity and asymmetry profiles.

The refraction at the surface barrier has strong effects in the case of large polar angles and low kinetic energies. Therefore, the strongest effects due to ΔE have to be expected for intensity and asymmetry profiles that show pronounced angular-dependent structures for large polar angles and a strong energy dependence of these structures.

EXPERIMENT AND CALCULATIONS

The experimental setup is described elsewhere.[18,19] Here the main points are sketched briefly. A spin-polarized electron beam from a negative electron affinity (NEA) GaAS photoemission source[20,21] is diffracted at the target crystal, and the spin-dependent intensities are recorded in different beams (Fig. 3). The degree of the spin polarization of the electrons emitted from the GaAs source is $0.26+0.03/-0.02$. The surface normal $\mathbf{n}$ of the target is chosen to lie in the scattering plane which is defined by the momentum of the incoming beam $\mathbf{k}_i$ and the momentum of the outgoing diffracted beam $\mathbf{k}_d$. The spin-polarization vector $\mathbf{P}_0$ of the incident electron beam

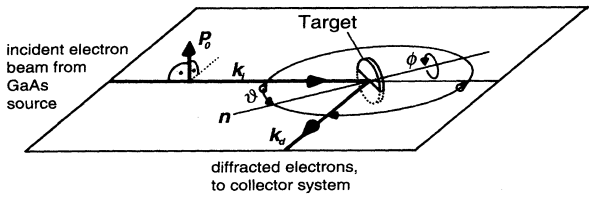

FIG. 3. Schematic view of the scattering geometry used in the experiment.

is aligned normal to the scattering plane. $\mathbf{P}_0$ is switched between the two normal directions $(+,-)$ by switching the helicity of the circularly polarized light incident on the GaAs crystal. For each of these two directions of $\mathbf{P}_0$ the intensity of the outgoing beam is measured by a movable Faraday collector system with retarding grids to suppress inelastically scattered electrons. The spin-dependent intensities I_+ and I_- yield the scattering asymmetry $A_\perp$, which is the component of the asymmetry vector normal to the scattering plane:

$$A_\perp := \frac{1}{|\mathbf{P}_0|}\frac{I_+ - I_-}{I_+ + I_-} . \tag{4}$$

The target can be rotated about its surface normal and about a polar axis lying in the surface and perpendicular to the scattering plane. The asymmetry is measured as a function of the polar angle ϑ, which is the angle between the incoming beam and the surface normal $\mathbf{n}$ of the target crystal.

The substrate, a Pt(111) surface, is cleaned by ion bombardment and heating in oxygen. The Xe(111) crystal was grown by exposing the clean Pt(111) surface to 310 L Xe at about 35 K. After the preparation the diffraction pattern is a Xe(111) pattern. LEED spots arising from the substrate crystal are no longer visible.

The self-energy correction ΔE and the real part V_{0r} of the inner potential are investigated by comparing the measured angular-dependent asymmetry and intensity profiles with corresponding calculated profiles. The calculations have been performed using a relativistic LEED program. An overview of spin-polarized LEED (SPLEED) theory is given in Ref. 22; details of the program used are described in Ref. 18. The Xe core potential has been taken from standard (scalar relativistic) ASW (augmented spherical waves) band-structure calculations based on DFT LDA.[23]

For a correct description of SPLEED from Xe(111), the coexistence of domains of different stacking orders *ABC* and *ACB* in Xe(111) has to be taken into account.[24] A change of the stacking order from *ABC* to *ACB* is equivalent to a rotation of the crystal by $\Delta\phi = 60°$ around the surface normal. The primary beam is diffracted at both types of crystallites with the same probability. Therefore, the spin-dependent intensities of the diffracted beams generally have to be calculated for both azimuthal angles ϕ and $\phi + 60°$. The spin-dependent intensities for ϕ and $\phi + 60°$ are added separately for each of the two spin directions, and the scattering asymmetry is recalculated from the resulting spin-dependent intensities.

For some special cases the symmetry properties of the (111) surface of a fcc crystal reduce the computational effort considerably (see Fig. 4). Since the asymmetry vector is an axial vector, the component normal to the scattering plane $A_\perp$, which is measured in this experiment, is invariant under mirror operation at the mirror planes of the target.[22,25–27] The pseudomirror planes (dashed lines) can be transformed one into the other by a mirror operation at the mirror planes (solid lines). Therefore, it is not necessary to take into account the coex-

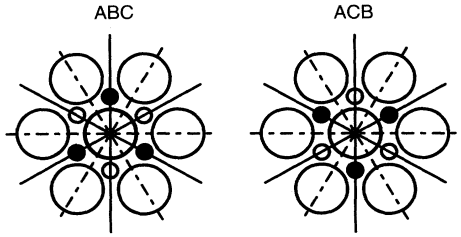

FIG. 4. Azimuthal orientation of the surface depending on the stacking order: *ABC* (left) and *ACB* (right). Large circles: surface layer; ●: second layer; ○: third layer. Solid lines: mirror planes; dashed lines: pseudo-mirror planes.

istence of crystallites of different stacking orders in the calculations, provided that the scattering plane is a pseudomirror plane. This consideration is only valid in the case of a primary beam with a spin-polarization vector normal to the scattering plane, as it is in the present experimental setup.

In contrast, for the nonspecular beams in the innermost ring the scattering plane is not a pseudomirror plane and therefore in the calculations account must be taken of the threefold symmetry of Xe(111) and the coexistence of domains of different stacking order. Because a change in the stacking order from *ABC* to *ACB* is equivalent to a rotation around the azimuthal angle by 60°, here the asymmetry profiles of two nonequivalent nonspecular beams of the innermost ring have to be calculated.

In the calculated asymmetry profiles the absolute values of the scattering asymmetry are generally found to be higher than in the measured asymmetry profiles. The reason is a background of elastically diffuse scattered electrons in the experiment. Due to this background the deep minima of the intensity present in the calculations are filled up in the measurements. Thus for the comparison of measured and calculated asymmetry profiles a background correction has to be applied to the measured data. The background is taken to be constant and spin independent, because its dependence on the polar angle, on the azimuthal angle, on the scattering energy, and on the spin direction cannot be quantified. The background intensity is subtracted from the spin-dependent intensities I_+ and I_-, and the scattering asymmetry is recalculated. The effect of the background correction is shown in Fig. 5.

To estimate the agreement between calculated and measured asymmetry and intensity profiles, the metric r factors R_I (intensity) and R_A^N (asymmetry) were used:[18,19,28]

$$R_I=\frac{1}{N_I}\sum_n |I_n^{\text{expt}}-S_I I_n^{\text{calc}}|,\quad N_I=\sum_n I_n^{\text{expt}},$$

$$S_I=\sum_n I_n^{\text{expt}}\Big/\sum_n I_n^{\text{calc}},$$

$$R_A^N=\frac{1}{N_A}\sum_n |A_n^{\text{expt}}-A_n^{\text{calc}}|,\quad N_A=\sum_n |A_n^{\text{expt}}|.$$

I_n^{expt} and I_n^{calc} denote the measured and calculated intensity at the nth data point, and A_n^{expt} and A_n^{calc} denote the corresponding asymmetries. S_I is a scaling factor, taking into account that no absolute intensities are measured. The sums run over all data points n. Because the elastic diffuse background affects the absolute value of the measured scattering asymmetry, in addition to the asymmetry r factor R_A^N (called the "normalized asymmetry r factor" in the following), another asymmetry r factor is used. This r factor (called the "scaled asymmetry r factor" in the following) is defined by

$$R_A^S=\frac{1}{N_A}\sum_n |A_n^{\text{expt}}-S_A A_n^{\text{calc}}|,\quad N_A=\sum_n |A_n^{\text{expt}}|,$$

$$S_A=\sum_n A_n^{\text{expt}}\Big/\sum_n A_n^{\text{calc}}$$

Due to the scaling factor S_A, R_A^S is less sensitive to the

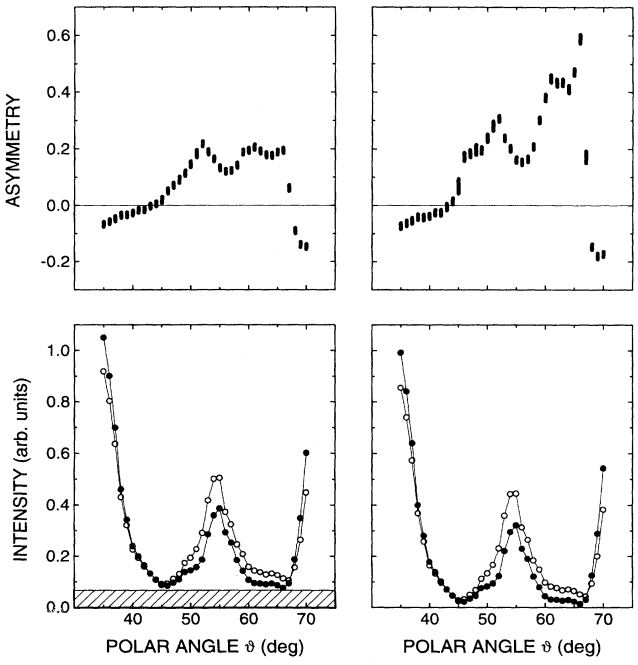

FIG. 5. Effect of background correction. Left: original data; right: background-corrected data. The data are measured in the specular beam of Xe(111) at a scattering energy of 56.5 eV in a pseudomirror plane. The dashed area in the intensity profile denotes the spin-independent background intensity. The magnitude of the symbols ● and ○ denoting the spin-dependent intensities I_+ and I_- in the intensity profiles is approximately 50 times larger than the statistical error of the measurement. In the measured asymmetry profiles the bar length represents the statistical errors. In addition, a scaling error of +7.5%-12.5% due to the uncertainty of the spin polarization of the primary beam has to be taken into account. Additional experimental uncertainties are energy ±1 eV, polar angle ±1.5°, and azimuthal angle ±0.5°. The scattering energy is the kinetic energy of the incident electron beam.

absolute values of the asymmetry compared with R_A^N. Its sensitivity to the structures of the profiles, i.e., the relative values and positions of maxima and minima of the scattering asymmetry, however, is enhanced. Using R_A^S for the comparison of measured and calculated asymmetry profiles is reasonable in the case when the asymmetries in the measured profiles are reduced by a background of diffuse scattered electrons. Consequently, R_A^S and R_A^N are applied to compare calculated results with original and with background-corrected measured asymmetry profiles, respectively.

RESULTS AND DISCUSSION

Figure 6 shows measured asymmetry profiles of the specular beam of Xe(111) in the energy range between 50.5 and 66.5 eV which are not background corrected. According to the previous discussion, the pronounced dependence on the polar angle and on the energy of the measured scattering asymmetry in the energy range from 54.5 and 62.5 eV qualifies these asymmetry profiles especially for the analysis of effects due to many-body interactions.

To investigate many-body effects, in the calculations the self-energy correction ΔE, the real part V_{0r} and the imaginary part V_{0i} of the inner potential were varied. The nearest-neighbor distance in the Xe crystal was kept constant at 4.37 Å.[29]

The systematic and independent variation of all three parameters ΔE, V_{0r} and V_{0i} yields best agreement between measurements and calculations for $\Delta E = 3.0$ eV, $V_{0r} = 3.0$ eV, and $V_{0i} = 2.0$ eV. This results from visual inspection as well as from r-factor analysis.

For example, Fig. 7 shows the comparison of a mea-

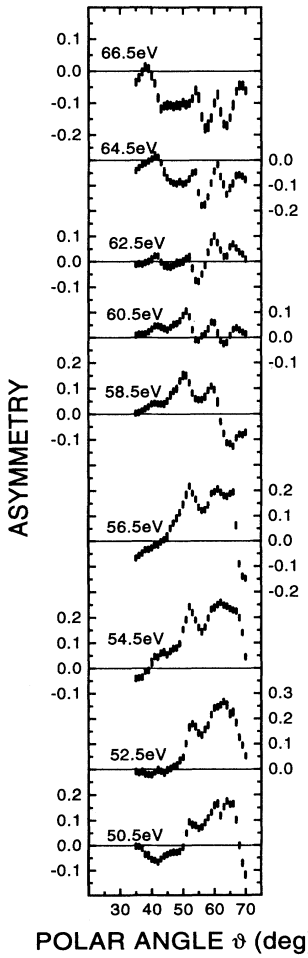

FIG. 6. Polar-angle-dependent asymmetry profiles of the specular beam of Xe(111) for different scattering energies measured in a pseudomirror plane. For experimental errors, see Fig. 5.

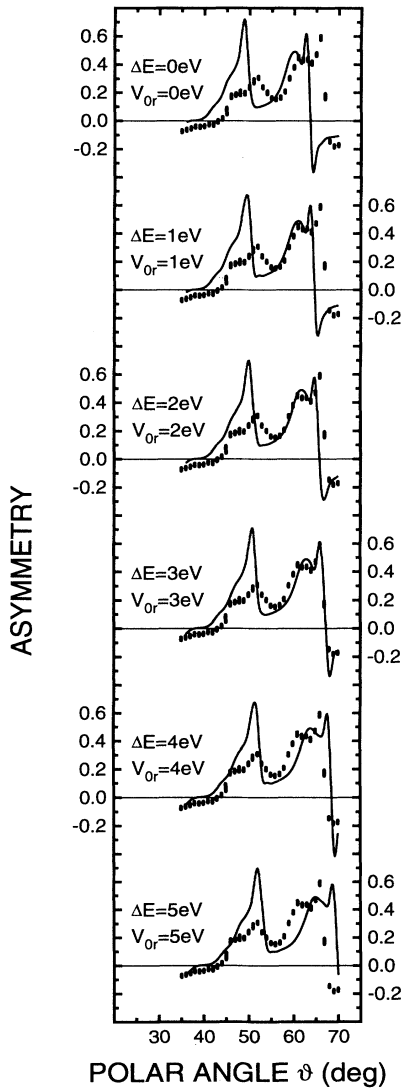

FIG. 7. Measured background-corrected asymmetry profile in comparison with calculated asymmetry profiles of the specular beam of Xe(111) in a pseudomirror plane for different values of ΔE and V_{0r}. The kinetic energy in the measurement is 56.5 eV. In the calculation E_{MT} is kept constant at 56.5 eV, ΔE and V_{0r} are varied such that $\Delta E = V_{0r}$. $V_{0i} = 2.0$ eV. For experimental errors, see Fig. 5.

sured asymmetry profile of the specular beam of Xe(111) with the corresponding asymmetry profiles calculated for different ΔE with E_{MT} kept constant, i.e., $\Delta E - V_{0r} = \text{const}$. The measured asymmetry profile is background corrected as outlined previously, the scattering energy is $E_{expt} = 56.5$ eV. As E_{MT} is constant, the overall structure of the calculated asymmetry profile does not change. The angular positions of the structures, however, are shifted due to the changing refraction at the surface barrier depending on the variation of V_{0r}. This shift is most pronounced for large polar angles.

For $\Delta E = 3.0$ eV and $V_{0r} = 3.0$ eV the agreement between calculation and experiment is quite good. All structures in the whole range of the polar angle are reproduced by the calculation. Very good agreement is found for polar angles between $\vartheta = 55°$ and 70°. The angular positions of the structures appearing here are strongly energy dependent and are thus well suited for investigating many-body effects. The structure of the maximum at $\vartheta = 50°$ is not that well reproduced. This maximum corresponds to a minimum of the intensity which is not found in the measurement (see Fig. 8). However, due to its angular position the calculated asymmetry profile is enveloping the maximum at $\vartheta = 50°$ and its shoulder at $\vartheta = 45°$.

Figure 9 shows the different r factors corresponding to Fig. 7, and their dependence on ΔE. The visual agreement between measurement and calculation is confirmed by the r-factor analysis. All r factors have a minimum at $\Delta E = 3.0$ eV and $V_{0r} = 3.0$ eV in common. Due to the experimental errors in the determination of the polar angle of $\pm 1.5°$ and of the energy of ± 1.0 eV, an error of ± 1.5 eV in the determination of ΔE and V_{0r} has to be taken into account.

The intensity profile corresponding to the asymmetry profile at $\Delta E = 3.0$ eV and $V_{0r} = 3.0$ eV is shown in Fig. 8. With respect to the intensity, measurement and calculation agree quite well too. Although the angular positions of the maximum at $\vartheta = 55°$ differ by 1.5° between the calculated and measured asymmetry profiles, the angular position of the steep increase in the intensity at $\vartheta = 70°$ and the steep decrease at $\vartheta = 40°$ and the structure of the measured intensity profile as a whole are well reproduced by the calculation.

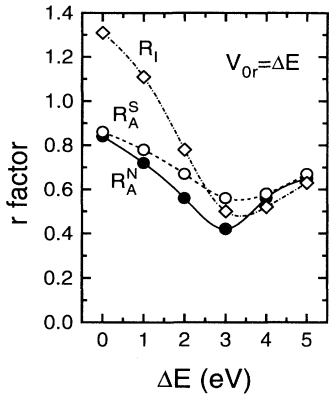

FIG. 9. r factors R_A^N (●), R_A^S (○), and R_I (◇) of the comparison of measured and calculated asymmetry and intensity profiles for the specular beam of Xe(111) as a function of ΔE with $\Delta E = V_{0r}$ (also see Fig. 7). Scattering energy: 56.5 eV, $V_{0i} = 2.0$ eV.

Figure 10 shows calculated and measured asymmetry and intensity profiles at a different energy $E_{expt} = 66.5$ eV. In this example only those calculated profiles yielding the best agreement are shown, which is also achieved for $\Delta E = 3.0$ eV and $V_{0r} = 3.0$ eV. The asymmetry profiles show a good agreement with respect to the value of the asymmetry and the position of the maxima, and also with respect to the structure of the profile as a whole. The same holds for the intensity. Although the maximum in the measured intensity profile at $\vartheta = 60°$ differs slightly

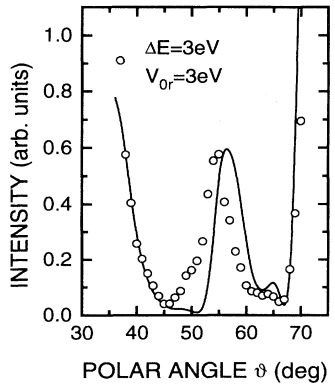

FIG. 8. Measured and calculated intensity profiles of the specular beam of Xe(111) in a pseudomirror plane for $\Delta E = V_{0r} = 3.0$ eV. Scattering energy: 56.5 eV, $V_{0i} = 2.0$ eV. For experimental errors, see Fig. 5.

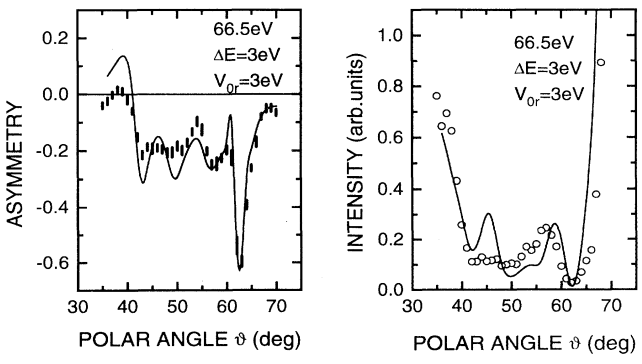

FIG. 10. Measured and calculated asymmetry and intensity profiles of the specular beam of Xe(111) in a pseudomirror plane for $\Delta E = V_{0r} = 3.0$ eV. The measured asymmetry profile is background corrected. Scattering energy: 66.5 eV, $V_{0i} = 2.0$ eV. For experimental errors, see Fig. 5.

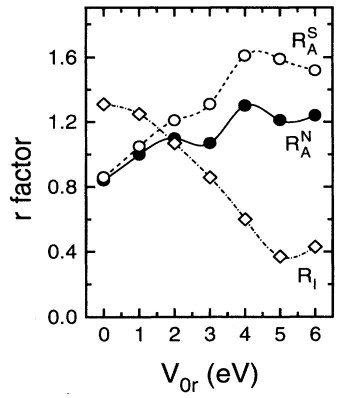

FIG. 11. r factors R_A^N (●), R_A^S (○), and R_I (◇) of the comparison of measured and calculated asymmetry and intensity profiles of the specular beam of Xe(111) as a function of V_{0r} for $\Delta E = 0.0$ eV. The measured asymmetry profiles are background corrected. Scattering energy: 56.5 eV, $V_{0i} = 2.0$ eV.

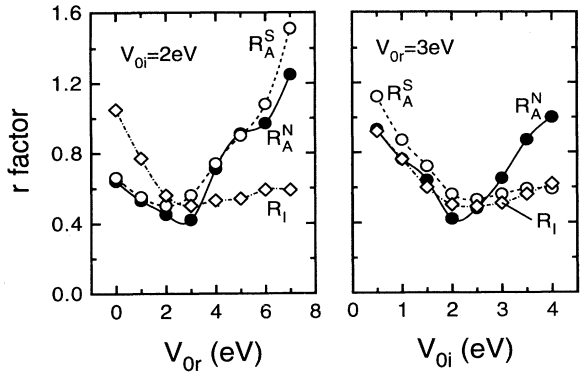

FIG. 13. r factors R_A^N (●), R_A^S (○), and R_I (◇) of the comparison of measured and calculated asymmetry and intensity profiles of the specular beam of Xe(111) as a function of the real part V_{0r} and the imaginary part V_{0i} of the inner potential. The measured asymmetry profiles are background corrected. Scattering energy: 56.6 eV, $\Delta E = 3.0$ eV.

from the calculation, and although in the calculation there is a small maximum at $\vartheta = 45°$ which is not seen in the experiment, the angular position of the steep increase in the intensity at $\vartheta = 65°$ and the steep decrease at $\vartheta = 40°$ and the structure of the measured profile as a whole are well reproduced by the calculation.

Achieving a good agreement between calculation and experiment by changing the refraction at the surface barrier alone, which is determined by V_{0r}, is not possible. Especially the inclusion of the spin dependence of the diffraction process appears to be advantageous in the separation of both the effects due to the self-energy correction ΔE and the effects due to the real part V_{0r} of the inner potential. Intensity measurements alone do not lead to clear results; they might even be misleading. Varying V_{0r} alone (vanishing self-energy correction, $\Delta E = 0$ eV) results in the r factors shown in Fig. 11. The asymmetry r factors increase with increasing V_{0r}. The contrary behavior of the intensity r factor is remarkable: in contrast to the asymmetry r factors, the intensity r factor decreases with increasing V_{0r} and has a minimum at $V_{0r} = 5.0$ eV, even deeper than at $\Delta E = 3.0$ eV and $V_{0r} = 3.0$ eV (see Fig. 9). The corresponding asymmetry and intensity profiles are shown in Fig. 12. The measured and calculated intensity profiles exhibit a good agreement comparable to those shown in Fig. 8, but no agreement at all can be found for the asymmetry profiles. Thus varying V_{0r} alone does not lead to an agreement between calculation and experiment.

Besides the real part V_{0r}, the imaginary part V_{0i} of the

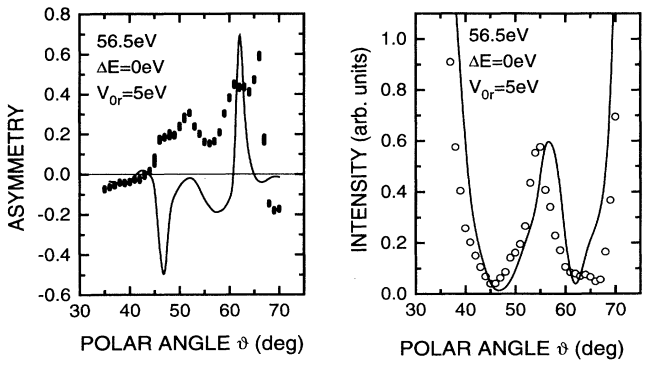

FIG. 12. Comparison of measured and calculated asymmetry and intensity profiles of the specular beam of Xe(111) in a pseudomirror plane $V_{0r} = 5.0$ eV and $\Delta E = 0.0$ eV. Scattering energy: 56.5 eV, $V_{0i} = 2.0$ eV. The measured asymmetry profile is background corrected. For experimental errors, see Fig. 5.

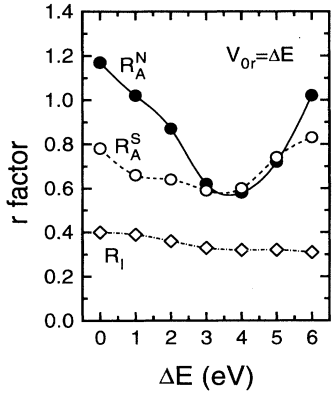

FIG. 14. r factors R_A^N (●), R_A^S (○), and R_I (◇) of the comparison of measured and calculated asymmetry and intensity profiles of the (10) beam of Xe(111) as a function of ΔE with $\Delta E = V_0$. The measured asymmetry profiles are background corrected. The kinetic energy in the measurement is 64.5 eV, and in the calculation E_{MT} is kept constant at 64.5 eV. $V_{0i} = 2.0$ eV.

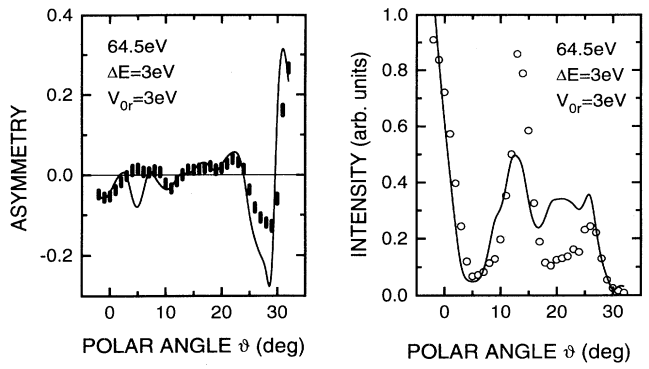

FIG. 15. Comparison of measured and calculated asymmetry and intensity profiles of the (10) beam of Xe(111) with $V_{0r}=\Delta E=3.0$ eV. The measured asymmetry profile is background corrected. Scattering energy: 64.5 eV, $V_{0i}=2.0$ eV. For experimental errors, see Fig. 5.

inner potential also affects the SPLEED calculation as another nongeometrical parameter. Figure 13 shows the dependence of the r factors on V_{0r} and V_{0i} for $\Delta E=3.0$ eV. For the real part the r factors have a minimum at $V_{0r}\cong 3.0$ eV in common, for the imaginary part the minimum of the r factors is located at $V_{0i}\cong 2.0$ eV. Thus the inner potential is determined to be $V_{0r}=3.0\pm 1.5$ eV and $V_{0i}=2.0\pm 0.5$ eV.

In order to test these results, a corresponding investigation for a nonspecular beam of Xe(111), the (10) beam, has been carried out. Figure 14 shows the r factors of the comparison of calculated and measured asymmetry and intensity profiles for this nonspecular beam. The measured data are background corrected. The scattering energy in the measurement is $E_{\text{expt}}=64.5$ eV. In the calculation E_{MT} is kept constant at a value of 64.5 eV, and ΔE and V_{0r} are varied accordingly. Both asymmetry r factors show a common minimum between $\Delta E=3.0$ eV and $\Delta E=4.0$ eV, confirming the results obtained for the specular beam. The slight difference of the values of ΔE and V_{0r} compared with the values found for the specular beam are within the experimental uncertainties. The structureless intensity r factor is of no use for the determination of the self-energy correction in this case. However, the low values of this r factor show the reliability of the calculation.

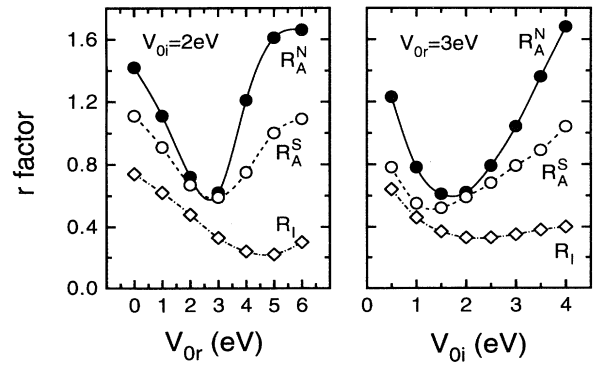

FIG. 16. r factors R_A^N (●), R_A^S(○), and R_I (◇) of the comparison of measured and calculated asymmetry and intensity profiles of the (10) beam of Xe(111) as a function of the real part V_{0r} and imaginary part V_{0i} of the inner potential. The measured asymmetry profiles are background corrected. Scattering energy: 64.5 eV, $\Delta E=3.0$ eV.

The asymmetry and intensity profiles connected with the r-factor minimum at $\Delta E=3.0$ eV and $V_{0r}=3.0$ eV are shown in Fig. 15. Calculation and experiment agree well with respect to the asymmetry as well as to the intensity. Although the ratio of the maxima at $\vartheta=10°$ and 25° is not correctly reproduced by the calculated intensity profile, the angular positions of the maxima and minima and the structure of the measured intensity profile as a whole are well described by the calculation.

The r factor's dependence on V_{0r} and V_{0i} at $\Delta E=3.0$ eV is shown in Fig. 16. In good agreement, the asymmetry r factors show a common minimum for the real part V_{0r} of the inner potential at about $V_{0r}\cong 3.0$ eV, and the intensity r factor has a flat minimum between $V_{0r}=4.0$ eV and $V_{0r}=5.0$ eV. For the imaginary part V_{0i} of the inner potential the asymmetry r factors show a minimum at $V_{0i}=1.5$–2.0 eV, the intensity r factor at $V_{0i}=2.0$–2.5 eV. Thus the values for the inner potential of $V_{0r}=3.0\pm 1.5$ eV and $V_{0i}=2.0\pm 0.5$ eV found in the analysis of the specular beam are confirmed.

CONCLUSION

The comparison between measured and calculated asymmetry and intensity profiles of the specular beam and of the nonspecular (10) beam from Xe(111) shows significantly the necessity to include many-body interactions in (SP)LEED theory. Only by including a constant self-energy correction $\Delta E=3.0\pm 1.5$ eV can good agreement between measured and calculated data be achieved. Satisfactory agreement between measurement and calculation, however, cannot be achieved, if only the real part V_{0r} of the inner potential is taken into account. The value of the self-energy correction ΔE found in this study agrees well with the difference of approximately 3 eV between the width of the fundamental band gap predicted by band-structure calculations based on DFT-LDA (Refs. 11-13) and the width determined experimentally by optical reflection and absorption measurements,[14–17] and with the self-energy correction $\Delta E=3.15$ eV found in a photoemission study.[11] The inner potentials were determined to be $V_{0r}=3.0\pm 1.5$ eV and $V_{0i}=2.0\pm 0.5$ eV. The errors of ΔE, V_{0r}, and V_{0i} are mainly due to the uncertainty in the determination of the polar angle and the energy in the experiment.

The values for the inner potential are contrary to a previous LEED analysis[30] which resulted in $V_{0r}=10$ eV and $V_{0i}=4$ eV. However, that work was based on a kinematic model, which has been shown to be completely insufficient for the description of LEED from Xe(111).[24]

Especially the inclusion of the spin dependence of the diffraction process appears to be advantageous for the separation of both the effects due to the self-energy correction and the effects due to the inner potential, since with respect to the intensity and the asymmetry agreement between measurements and calculations has to be achieved simultaneously. Analyzing only the intensity of the diffracted beams does not lead to clear results and may even be misleading.

Effects due to the self-energy correction ΔE are most pronounced in a diffraction geometry using grazing angles, since in this case a self-energy correction ΔE cannot be compensated for by the real part of the inner potential in the calculation without severely affecting the angular positions of the structures in the profiles. In conventional LEED studies a diffraction geometry with almost normal incidence is used, and energy-dependent measurements are performed. For almost normal incidence the refraction at the surface barrier almost vanishes. Under these conditions the observation of a self-energy correction ΔE is impossible. This explains why in conventional LEED studies all energy-correcting terms are included in the real part of the inner potential, and why a self-energy correction is not taken into account, and, moreover, why it is not necessary to take into account a self-energy correction in this special diffraction geometry.

Finally we would like to point out that the objective of our SPLEED study has not been a geometrical structure determination but an investigation of important parameters characterizing the electronic structure of a solid surface. Usually it is the electronic structure in the vicinity of the Fermi energy that is the subject of interest. Less interest has been focused on the electronic states well above the vacuum level up to now. These high-energetic states, however, are inevitably involved in spectroscopies studying the electronic structure around the Fermi energy, i.e., photoemission and inverse photoemission spectroscopy. LEED provides an independent method of studying the high-energetic scattering states, thereby contributing to a better understanding of the electronic structure and, as shown here, especially of many-body effects at solid surfaces.

ACKNOWLEDGMENT

Financial support by the Deutsche Forschungsgemeinschaft within the Sonderforschungsbereich 216 is gratefully acknowledged.

---

*Author to whom correspondence should be addressed. Present address: PTB Braunschweig, D-38116 Braunschweig, Germany.

†Present address: Institut für Physik, Humboldt-Universität zu Berlin, D-10099 Berlin, Germany.

[1]G. Capart, Surf. Sci. **13**, 361 (1969).

[2]P. J. Estrup and E. G. McRae, Surf. Sci. **25**, 1 (1971).

[3]J. B. Pendry, *Low Energy Electron Diffraction* (Academic, London, 1974).

[4]M. B. Webb and M. G. Lagally, in *Solid State Physics,* edited by H. Ehrenreich, F. Seitz, and D. Turnbull (Academic, New York, 1973), Vol. 28, p. 301.

[5]R. C. Jaklevic and L. C. Davis, Phys. Rev. B **26**, 5391 (1982).

[6]M. Lindroos, H. Pfnür, and D. Menzel, Phys. Rev. B **33**, 6684 (1986).

[7]A. Liebsch, Phys. Rev. Lett. **43**, 1431 (1979).

[8]A. Liebsch, Phys. Rev. B **23**, 5203 (1981).

[9]P. A. Bennett, J. C. Fuggle, F. U. Hillebrecht, A. Lenselink, and G. A. Sawatzky, Phys. Rev. B **27**, 2194 (1983).

[10]W. Borgiel and W. Nolting, Z. Phys. B **78**, 241 (1990).

[11]B. Kessler, A. Eyers, K. Horn, N. Müller, B. Schmiedeskamp, G. Schönhense, and U. Heinzmann, Phys. Rev. Lett. **59**, 331 (1987).

[12]N. C. Bacalis, D. A. Papaconstantopoulos, and W. E. Pickett, Phys. Rev. B **38**, 6218 (1988).

[13]U. Rössler, in *Rare Gas Solids I,* edited by M. L. Klein and J. A. Venables (Academic, London, 1976), p. 505.

[14]G. Baldini, Phys. Rev. **128**, 1562 (1962).

[15]R. Haensel, G. Keitel, E. E. Koch, M. Sobowski, and P. Schreiber, Opt. Commun. **2**, 59 (1970).

[16]S. J. Scharber, Jr. and S. W. Webber, J. Chem. Phys. **55**, 3985 (1971).

[17]B. Sonntag, in *Rare Gas Solids II,* edited by M. L. Klein and J. A. Venables (Academic, London, 1977), p. 1021.

[18]M. Potthoff, G. Hilgers, N. Müller, U. Heinzmann, L. Haunert, J. Braun, and G. Borstel, Surf. Sci. **322**, 193 (1995).

[19]G. Hilgers, M. Potthoff, N. Müller, and U. Heinzmann, Surf. Sci. **322**, 207 (1995).

[20]D. T. Pierce and F. Meier, Phys. Rev. B **13**, 5484 (1976).

[21]D. T. Pierce, R. J. Celotta, G.-C. Wang, W. N. Unertl, A. Galejs, C. E. Kuyatt, and S. R. Mielszarek, Rev. Sci. Instrum. **51**, 478 (1980).

[22]R. Feder, J. Phys. C **14**, 1049 (1981).

[23]M. Timmer and G. Borstel (private communication).

[24]G. Hilgers, Ph.D. thesis, Universität Bielefeld, 1992.

[25]B. I. Dunlap, Solid State Commun. **35**, 141 (1980).

[26]R. Feder, Phys. Lett. **78A**, 56 (1980).

[27]P. Bauer, R. Feder, and N. Müller, Solid State Commun. **36**, 249 (1980).

[28]G. Kleinle, W. Moritz, and G. Ertl, Surf. Sci. **238**, 119 (1990).

[29]R. W. G. Wyckoff, *Crystal Structures II* (Interscience, New York, 1964).

[30]A. Ignatjevs, J. B. Pendry, and T. N. Rhodin, Phys. Rev. Lett. **26**, 189 (1971).